



Title	Damage detection in membrane structures using non-contact laser excitation and wavelet transformation
Author(s)	Huda, Febliil; Kajiwara, Itsuro; Hosoya, Naoki
Citation	Journal of Sound and Vibration, 333(16), 3609-3624 https://doi.org/10.1016/j.jsv.2014.04.008
Issue Date	2014-08-04
Doc URL	http://hdl.handle.net/2115/56997
Type	article (author version)
File Information	JSV333-16 3609-3624.pdf



[Instructions for use](#)

Damage Detection in Membrane Structures Using Non-contact
Laser Excitation and Wavelet Transformation

Febliil Huda^{#1}, Itsuro Kajiwara^{#2}, Naoki Hosoya^{#3}

#1

Graduate Student

Division of Human Mechanical Systems and Design, Hokkaido University

N13, W8, Kita-ku, Sapporo 060-8628, Japan

Phone: +81-11-706-6392, Fax. +81-11-706-6390

E-mail: feblilhuda@ec.hokudai.ac.jp

Junior Lecturer

Department of Mechanical Engineering, University of Riau

Kampus Bina Widya, Jl. HR Subrantas km 12,5 Pekanbaru 28293, Riau, Indonesia

#2 (Corresponding author)

Professor

Division of Human Mechanical Systems and Design, Hokkaido University

N13, W8, Kita-ku, Sapporo 060-8628, Japan

Phone: +81-11-706-6390, Fax. +81-11-706-6390

E-mail: ikajiwara@eng.hokudai.ac.jp

#3

Associate Professor

Department of Engineering Science and Mechanics, Shibaura Institute of Technology

3-7-5 Toyosu, Koto-ku, Tokyo 135-8548, Japan

Phone: +81-3-5859-8055, Fax. +81-3-5859-8001

E-mail: hosoya@sic.shibaura-it.ac.jp

Abstract:

In this paper, a vibration testing and health monitoring system based on an impulse response excited by laser is proposed to detect damage in membrane structures. A high power Nd: YAG pulse laser is used to supply an ideal impulse to a membrane structure by generating shock waves via laser-induced breakdown in air. A health monitoring apparatus is developed with this vibration testing system and a damage detecting algorithm which only requires the vibration mode shape of the damaged membrane. Artificial damage is induced in membrane structure by cutting and tearing the membrane. The vibration mode shapes of the membrane structure extracted from vibration testing by using the laser-induced breakdown and laser Doppler vibrometer are then analyzed by 2-D continuous wavelet transformation. The location of damage is determined by the dominant peak of the wavelet coefficient which can be seen clearly by applying a boundary treatment and the concept of an iso-surface to the 2-D wavelet coefficient. The applicability of the present approach is verified by finite element analysis and experimental results, demonstrating the ability of the method to detect and identify the positions of damage induced on the membrane structure.

Keywords: Damage detection, Membrane structure, Laser-induced breakdown, Vibration mode shape, Continuous wavelet transformation

1. Introduction

Membranes are widely used in a number of fields of engineering as membranes are thin, light, flexible, and translucent. There are numerous existing practical applications of membrane structure in architectural and civil engineering structures, diaphragms in switches and transducers, biomedical prosthesis such as artificial arteries and organs, and space-based applications such as radio antennas, optical reflectors and solar sails. From this background, research into membrane structures has become an important research topic in mechanical engineering contributing to ensuring the proper functioning of membrane structures, and assessment of vibration of membrane structures is important and has been investigated for at least three centuries [1].

Vibrating membranes have been investigated with different types of excitation and vibration measurement methods. Because of the extreme flexibility and lightness of membranes, the standard methods of experimental modal analysis, like with attaching accelerometers and shaker stringers directly to a vibrating structure, cannot be used with membranes, as such techniques lead to non-negligible added mass and stiffness that influences and skews the results, making the use of non-contact measurement methods essential [1]. Chobotov investigated the non-linear vibration of membranes [2], with an experimental system using horn-acoustical excitation and employing a capacitance displacement sensor to measure the fundamental mode of circular Mylar membrane. Jenkins performed experiments using local excitation on low tensioned membranes [3,4] with loudspeaker to provide acoustic excitation and a laser vibrometer to measure the natural frequencies and mode shapes of circular Mylar polyester membrane. However, using acoustic exciters like horns and loudspeakers require attaching these exciters close to the vibrating structure. Loudspeakers may affect the characteristics of the sound field or placement may be difficult because of the shape and size of loudspeakers [5], and when producing acoustic excitation, the loudspeakers give a like-area excitation while point excitation is required for ideal vibration measurement. Kajiwara conducted experiments on membrane structures in vacuum using non-contacting laser excitation to excite membrane structures, and used laser Doppler vibrometer (LDV) to measure the vibration response [6]; however this method requires attaching light metal part at the point of excitation of the membrane structure to generate laser ablation adding mass and stiffness to the membrane.

Based on the above, those issues have led to research into acoustical excitation without any attachments to measured structures which permits some distance to the excited structure and gives the possibility of conducting experiments in small areas. Vibration test using laser-induced breakdown (LIB) involves no any attachments to measured structures, and offers the possibilities of applying acoustical excitation on a point with some distance between exciter and membrane structure, even in really small area.

In the research reported here, a vibration testing and health monitoring system based on an impulse response excited by laser is proposed to detect damage on membrane structures. A high power Nd: YAG pulse laser is used to generate an ideal impulse on the membrane structure by applying shock wave generated by LIB in air. A health monitoring apparatus is developed with this vibration testing set-up and a damage location detecting algorithm which only requires the vibration mode shape of the damaged membrane is developed. Artificially induced damages to membrane structure are provided by cutting and tearing the membrane. The vibration mode shapes of the membrane structure extracted from the vibration testing by LIB and LDV are analyzed by two-dimensional (2-D) continuous wavelet transformation (CWT). The effectiveness of the present approach is verified by finite element analysis (FEA) using ANSYS 14.0 and experimental results. Finally, a method for damage detection in membrane structures is proposed by applying 2-D CWT and an iso-surface concept to the membrane structure with different types of damage. The effectiveness of the present approach is verified by simulations and experiments.

2. Vibration testing system using LIB

2.1 Acoustic excitation by LIB

In this research, an excitation to a membrane structure is applied in the form of acoustic excitation achieved by generating an ideal point sound source at specific location via LIB which offers the possibility of conducting experiments with acoustic excitation in small and limited space. The LIB refers to the formation of plasma through the cascade process caused by electrons emitted from atoms and molecules that have absorbed multiple photons through a multi-photon process when a laser beam is focused in a gas. A portion of this plasma energy is transformed to a shock wave, which is the source of the sound generated by LIB.

In the vibration testing here, the acoustic excitation set-up is configured by combining a high power Nd: YAG pulse laser and a convex lens. By passing the laser beam through the convex lens which focuses the beam, the local intensity of the laser beam reaches to or above the minimum LIB threshold of 10^{15} W/m^2 [7-9]. The acoustic excitation uses force generated by this method is highly reproducible as it is defined by the specifications of the laser and the lens. The process to achieve acoustic excitation by LIB is presented in Fig. 1.

This system uses an Nd: YAG pulse laser (Surelite III, Continuum Inc., wavelength: 1064 nm, laser beam radius: 4.75 mm, pulse width: 5 ns, maximum output: 1 J), and a convex lens is placed on an optical table to focus the laser beam and generate the point sound source LIB. The set-up for the application of the acoustic excitation to a membrane structure by LIB is shown in Fig. 2, where the laser beam produced by Nd: YAG pulse laser passing through the convex lens, and the LIB then occurs at a point determined by the distance equal to the focal length of the convex lens. The LIB at

the point of focus generates the sound, and the sound excites the membrane, this phenomenon is termed acoustic excitation by LIB.

2.2 Measurement and analysis of the output

To measure the output response, two LDVs are set to obtain the responses of the membrane structure. One LDV is fixed to measure the response at the centre of the membrane, and the other is used for measuring the response at points along the membrane. These measurements enable the mode shapes of membrane to be determined. A spectrum analyzer (A/D; NI-4472B, Software; Catec CAT-System) is used for measuring the velocity response and analysing the Fourier spectrum of the structure. The vibration testing apparatus and arrangement for the membrane structure is shown in Fig.3.

2.3 Membrane structure setup

The membrane material is Kapton, manufactured by Du Pont-Toray Co., Ltd. Owing to its good resistance to temperature. Kapton is often used in actual space applications. The membrane here is 200 mm \times 200 mm and 50 μ m thick, with a mass density of 1420 kg/m³, Poisson ratio 0.29, and Young's modulus 3.4 GPa.

The membrane is clamped on four sides by metal clamps and kept stretched by three 700 gram masses and one side is fixed, the masses and the fixed side are connected to the metal clamps by steel wires. This membrane structure is supported by a base which is fixed to an optical table. To obtain the mode shapes of the membrane, the responses are measured at the intersections of 20 mm interval grid lines, giving 11 \times 11 points of measurement on the membrane.

3. 2-D CWT for damage detection in membrane structure

The 2-D CWT considered in this study is based on the formulation by Antoine [10], and wavelet computations are performed using MATLAB[®] and the YAWTb toolbox [11]. The procedure to detect the position of damage in the membrane structure is adopted from the procedure suggested by Fan [12], using the 2-D CWT derivative Gauss (Dergauss2d), which was used successfully for detecting damage on plates using mode shape data.

3.1 2-D CWT derivative Gauss

If there is a 2-D image/signal of $s(\vec{x}) \in L^2(\mathbb{R}^2, d^2\vec{x})$, its 2-D CWT (with respect to the wavelet ψ) $S(\vec{b}, a, \theta) \equiv T_\psi s$ is the scalar product of s with the transformed wavelet $\psi_{\vec{b}, a, \theta}$ and considered as a function of (\vec{b}, a, θ) as:

$$\begin{aligned}
S(\vec{b}, a, \theta) &\equiv \langle \psi_{\vec{b}, a, \theta}, s \rangle = a^{-1} \int_{\mathbb{R}^2} \overline{\psi(a^{-1} r_{-\theta}(\vec{x} - \vec{b}))} s(\vec{x}) d^2 \vec{x} \\
&= a \int_{\mathbb{R}^2} \overline{\hat{\psi}(a r_{-\theta}(\vec{k}))} e^{-i \vec{b} \cdot \vec{k}} \hat{s}(\vec{k}) d^2 \vec{k}
\end{aligned} \quad \dots (1)$$

where,

$S(\vec{b}, a, \theta)$ = wavelet coefficient of transformed signal

$\psi_{\vec{b}, a, \theta}$ = family of wavelet

\vec{b} = translation vector

a = scaling factor

θ = rotation angle

\vec{k} = Fourier transformation function

$r_{-\theta}$ = rotation matrix.

Gaussian filtering is a widely used approach to filter out the high frequency noises. In this case, the desired signal can be obtained by convolving the differentiated mode shape $s(x, y)$ with a Gaussian $g(x, y)$ as:

$$\tilde{s} = g(x, y) * \left(\frac{\partial}{\partial x} \right)^m \left(\frac{\partial}{\partial y} \right)^n s(x, y) \quad \dots (2)$$

where (*) denotes the convolution operator. The 2-D Gaussian is defined as

$$g(x, y) = \exp\left(-\frac{|\vec{x}|^2}{2\sigma^2}\right) = \exp\left(-\frac{x^2+y^2}{2\sigma^2}\right), \vec{x} = (x, y) \quad \dots (3)$$

Using the well-known property of convolution, the following equation is obtained

$$\tilde{s} = g(x, y) * \left(\frac{\partial}{\partial x} \right)^m \left(\frac{\partial}{\partial y} \right)^n s(x, y) = \left(\frac{\partial}{\partial x} \right)^m \left(\frac{\partial}{\partial y} \right)^n g(x, y) * s(x, y) \quad \dots (4)$$

When the derivative of a 2-D Gaussian as the mother wavelet is adopted and equation (1) is rewritten as a convolution, the equation becomes:

$$S(\vec{b}, a, \theta) \equiv (\psi_{a, \theta} * s)(\vec{b}) = \left(\left(\frac{\partial}{\partial x} \right)^m \left(\frac{\partial}{\partial y} \right)^n g_{a, \theta} * s \right)(\vec{b}) = \tilde{s}_{a, \theta}(\vec{b}) \quad \dots (5)$$

where $\left(\frac{\partial}{\partial x} \right)^m \left(\frac{\partial}{\partial y} \right)^n g_{a, \theta}$ is the Gaussian filter. Hence, the desired differentiated and filtered signal can be obtained by a 2-D wavelet transform of the original mode shape with the derivative of the 2-D Gaussian (Dergauss2d) as the wavelet.

Fan [11] suggested using $m = n = 2$ for damage detection, as it gives a more smooth result. In this paper, the above $m = n = 2$ parameters will be adopted to detect the position of damage on the membrane structure.

3.2 The procedure of damage detection on the membrane

The following procedure suggested by Fan [12] will be used to detect damage locations in the membrane structure:

- Step 1: Transforming the mode shape data by 2-D CWT. The 2-D CWT of the membrane mode shape is computed using the YAWTb toolbox [10] in a continuous scale variation.
- Step 2: Applying a boundary distortion treatment to wavelet coefficient. All the wavelet coefficients in the “boundary effect regions” are set to zero. With this treatment, damage at the edge of the membrane cannot be detected, and this paper is only concerned with detecting membrane damage in non-edge locations.
- Step 3: Calculating the threshold value. The maximum and minimum values of the updated wavelet coefficient are calculated. The largest absolute value is multiplied with a threshold ratio between 0 and 1 to generate a threshold value.
- Step 4: Generating the iso-surface graph. The points with the threshold values are connected to form an “iso-surface” connecting points of equal elevation with contour lines.

In this paper, the first principal mode shape of the membrane is employed to detect the position of damage, but other mode shapes at higher frequencies will be used to detect the damage if the damage cannot be detected by this first principal mode shape. This approach is based on the idea that the high amplitude at specific area of the mode shape of the damage could occur in higher frequency modes, and this mode shape shows the dominant peak of the position of the damage. Further, the present vibration testing method enables high frequency vibration measurements due to the non-contact excitation making it possible to detect the position of the damage on the membrane using higher order mode shapes.

4. FEA investigation of damage detection on the membrane structure

4.1 Model description

The finite element analysis software ANSYS 14.0 is used to conduct the pre-stress modal analysis to generate the mode shapes of normal and damaged membrane structures. The SHELL181 element of ANSYS is used to construct the physical model of the membrane, and the SOLID186 element is employed to model the clamps at the corners of the membrane. The contact between the membrane and the clamps is presented by surface-surface contact elements, pairs of elements, the contact element CONTA174 and target element TARGE170. Bonded type contacts are applied to each contact between the membrane and a clamp. The membrane is uniformly divided into approximately

10,000 $2\text{ mm} \times 2\text{ mm}$ four node membrane elements. The mode shapes are extracted from all 11×11 node data in the model. The finite element model of the membrane structure is shown in Fig.4.

Fig. 4 shows that the membrane is tightened by wires at the four corners, where each wire is modeled as a tension spring with a stiffness of 5000 N/m. Three wires are kept in tension by 700 gram masses, equivalent to 7 N of tension force, and one wire is pinned to the base.

The membrane is modeled in normal (without induced damage) and damaged conditions. The damaged conditions are achieved by cutting or tearing the membrane in specified forms and positions. The static structural analysis is conducted first, followed by the modal analysis. The results of static structural analysis are plotted as the initial condition of the modal analysis, and this is termed the pre-stress modal analysis. The mode shapes of the membrane structure are then calculated from the results of this analysis.

4.2 Analysis of the normal condition by simulation

To apply the damage detection approach to simulations, the normal condition of the membrane must first be established to validate the finite element model, without exposing the membrane any type of imposed damage. The process of the analysis of the membrane in the normal condition by simulation data is presented in Fig.5. The first principal modeshape (Fig.5(a)) is interpolated by cubic spline interpolation to get more data along the membrane (Fig.5(b)), and then processed by 2-D CWT, with scale $a = 2$ (Fig.5(c)). To get a clearer view of the state of the 2-D wavelet coefficient, the boundary treatment, removing large irregularities at the boundaries, needs to be applied (Fig.5(d)).

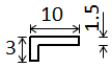
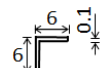
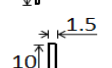
From wavelet coefficient with the boundary treatment obtained from the simulation data, it can be seen that there are peaks at the corners caused by the clamps; these do not arise from damage to membrane. The overall wavelet coefficient does not show any dominant peak for the wavelet coefficient, making it unnecessary for the next process to employ iso-surface generation.

4.3 Application of damage detection

To examine details of the results generated by the damage detection approach by 2-D CWT and FEM simulation, three different damage conditions were induced in the membrane finite element models. The Finite element model of the membrane with three damage scenarios are presented in Fig. 6, and details of the three damage cases are listed in Table 1.

There are two types of damage: cut and tear. The difference between cut and tear is that a cut requires removing some mass part of the membrane, while a tear does not remove any mass part of the membrane. The damage is simulated by pre-stress modal analysis and then the mode shapes are calculated from this analysis.

Table 1 Details of the damage induced on the membrane

Item	Damage type	Damage size (mm)	Closest measurement point (x,y) in mm
A	L-cut		(120,120)
B	L-tear		(140,100)
C	I-cut		(80,100)

The first principal mode shape of the membrane is employed to detect the position of the damage by applying the 2-D CWT and the iso-surface concept. When the position of the damage cannot be established by the first principal mode shape, higher order mode shapes that may appear at high frequency will be employed. This will be possible, because laser excitation offers the possibility of measurements at high frequency. The process of the analysis for detecting L-cut damage (A in Table 1) on the membrane by simulation data is shown in Fig.7.

To detect the L-cut damage on the membrane, the first principal mode shape data (Fig.7(a)) is used. The mode shape is then interpolated to obtain more data for the mode shape of the membrane (Fig.7(b)). The interpolated data of the mode shape is then analyzed using 2-D CWT, but the result still does not show the signature of the damage, because the results of the transformation have very high values on the corners and the edges of the 2-D wavelet coefficient (Fig.7(c)), this condition overwhelms the damage signature. To remove the effect of the high boundary values induced by the anchoring, the boundary treatment on wavelet coefficient data is implemented. From 2-D wavelet coefficient with the boundary treatment, scale $a = 2$, a dominant peak can be seen, and this may assumed to be the damage position (Fig.7(d)). The exact position of the damage can be verified by applying the iso-surface concept, where some of the treated 2-D wavelet coefficients from different scales (1-20) which have the same value range are connected to form surfaces, and the appearance becomes pointlike (Fig.7(e) and Fig.7(f)). The iso-surface for detecting L-cut position shows the damage position accurately similar to the damage scenario, where the closest measurement point is (120,120). These results allow the assumption that the FEA and damage detection approach using 2-D CWT works well in determining damage position on a membrane structure.

The same procedure as for detecting the L-cut is used to determine the position of the damage with L-tear (B in Table 1). The first principal mode shape is analyzed to detect the damage. The iso-surface view of the detected L-tear damage on the membrane by simulation data is shown in Fig.8. The iso-surface result detects the position (140,100) matching that of the damage scenario (Table 1).

For an I-cut damage (C in Table 1), the first principal mode shape cannot be used to detect the damage position, because the membrane stiffness at the measurement point closest to this damage scenario change very little, and the mode shape is very similar to the normal condition. The analysis of first principal mode shape for detecting the I-cut damage on the membrane by simulation data is shown in Fig. 9, where it can be seen that there are many peaks (the red contour region) in the treated 2-D wavelet coefficient, but there is no dominant peak. The peaks determined here suggest that something has happened to the membrane, and higher order modes need to be checked to fully understand the condition of the membrane.

The higher order mode shapes can be used to determine the position of the damage, and Fan used the fifth principal mode shape to establish the damage position on a plate [10]. Investigating higher frequency mode shapes, it is found that there is a mode shape which shows the existence of the dominant peak at frequency of 851 Hz. The mode shape at this frequency can be used to establish the position of the damage on the membrane structure. The analysis of higher order mode shape for detecting the I-cut damage on the membrane by simulation data is presented in Fig. 10. The iso-surface views show the position of the damage of the I-cut damage corresponding to the damage scenario.

5. Experimental verification of damage detection

5.1 Damage detection for single damage on membrane

To verify the applicability of the finite element analysis and to show the ability of damage detecting using laser excitation and wavelet transformation on a membrane, vibration testing on the membrane structure employed here using impulse excitation by LIB was conducted. The membrane structure was excited by acoustic excitation using the LIB, and the vibration responses were measured at the 11×11 points across the membrane. The frequency responses at all points of measurements were processed to show the mode shapes of the membrane by using MATLAB[®]. An example of the frequency response of the membrane in the normal (undamaged) condition at the center point of the membrane is presented on Fig. 11.

As Fig.11 shows, there are a large number of resonance peaks which explain the number of mode shapes of the membrane structure. The first natural frequency of the membrane is not the peak at the lowest frequency, but the peak with high amplitude response that is marked in Fig. 11. By further investigating the mode shapes of the membrane for these two peaks (the first and the marked peak), the first peak involves the deformation on tightening wires and clamps which means that it is not the proper membrane mode shape (rigid body of the membrane). The second peak as pointed in Fig. 11 does not reflect deformation of the wires and the clamps. The marked peak is the mode shape of the membrane alone, and will be used as the first principal mode shape of the membrane.

As the first step, the experiments are conducted by following the damage scenario (Table 1), single damage, as explained in section of 4.3. The Process of the analysis for detecting the L-cut damage (A in Table 1) on membrane by experimental data is presented in Fig. 12.

The procedure used for detecting the damage location using simulation data (detailed above) is implemented for the experimental data. Fig. 12 shows that the process of the analysis is using the first principal mode shape of the membrane (Fig. 12(a)). To get more point of data, the mode shape is interpolated (Fig. 12(b)), which are then transformed by 2-D CWT to get wavelet coefficient (Fig. 12(c)), and wavelet coefficients are then treated by the boundary treatment to get clearer contour of the wavelet coefficient (Fig. 12(d)) on the membrane. The position of the L-cut damage can be seen on the iso-surface view in 3-D ((Fig. 12(e)) and top view (Fig. 12(f)). The L-cut damage location on the membrane can be accurately detected, with good agreement between the experiment and simulation results. The location of the L-cut damage is shown at the position of (120,120) in Fig. 12.

The L-tear damage (B in Table 1) determination also uses the first principal mode shape, the iso-surface view of the detected L-tear damage on the membrane by experimental data are presented in Fig.13, which agrees with the simulation. Here, the noise additional to the point of the damage appearing as a small point (left panel in Fig. 13) can be ignored, because it is much smaller than the point at the damage position.

The I-cut damage type (C in Table 1), can not be determined by only the analysis with the first principal mode shape. This condition requires the use of higher frequency mode shapes, and it was found that in the higher frequency modes the damaged part appears as a high amplitude in the mode shape. By determining the mode shape at higher frequency, the damage position can be established. To detect a case with I-cut damage, a higher order mode shape with high local amplitude appears at frequency of 843.8 Hz (similar to FEM simulation). The analysis of higher order mode shape for detecting the I-cut damage on the membrane by experimental data is presented in Fig. 14. From Fig. 14, it can be seen that there is a dominant peak in the mode shape (Fig. 14(a)). This peak can also be seen clearly on the wavelet coefficient with boundary treatment by the scale $a = 2$ (Fig. 14(b)). Finally, on the iso-surface view (Fig. 14(c) and (d)), the exact position can be determined, and it corresponds to the damage scenario.

From the damage detection on the membrane structure involving the higher frequency mode shape, it can be assumed that using the higher frequency mode is effective to detect damage positions on the membrane structure. This allows the conclusion that using laser excitation to excite membrane structure in vibration testing is appropriate, because vibration testing using laser excitation provides the high frequency vibration data [6,13-16].

5.2 Damage detection for two damages on membrane

The damage detection method for membrane structures was also attempted with two places of damage on the membrane. Here, an I-cut and a square-hole were introduced in the membrane. The I-cut damage was $10 \text{ mm} \times 1.5 \text{ mm}$, and the square-hole was $10 \text{ mm} \times 10 \text{ mm}$. These positions of the damage on the membrane are shown in Fig. 15. These types of damages in these dimensions cannot be determined well using the first principal mode shape and the higher order mode approach will be used.

Vibration testing using laser excitation was performed on the membrane, and the mode shape containing dominant peaks of the two types of damages was found at the natural frequency of 799.1 Hz. The Process of the analysis for detecting I-cut & square-hole damage on the membrane by experimental data is presented in Fig. 16.

The mode shape at high frequency of 799.1 Hz shows two dominant peaks which may be predicted to be the position of damage (Fig. 16(a)). The wavelet coefficient with the boundary treatment (Fig. 16(b)) also shows the same situation with the peaks. Finally, the iso-surface views (Fig. 16 (c) and (d)) determine the two positions of damage which correspond to the positions of the induced damages.

When the mode shape change is evaluated by the frequency response of the membrane, it shows the corresponding resonance peak in the normal membrane condition. The frequency response without induced damage and condition with damage in two places (by the I-cut and square-hole, Fig.15) is shown in Fig. 17. Here, the resonance peaks for the normal and damaged conditions show that the peak in the frequency response of the normal condition corresponds to a resonance peak used in damage detection. In the normal condition, the initial resonance peak is at 801.6 Hz, and after introducing the two points of damage to the membrane, the resonance peak has shifted to 799.1 Hz. The mode shape at this frequency is used for detecting the position of the two locations of damage. It is commonly observed in structures, that damage which removes some part of the mass of the structure also reduces the stiffness, and the stiffness reduction shifts the resonance peaks to the lower frequencies. To verify that these two resonance peaks correspond to each other, the mode shape of the two conditions were compared, and the plots are shown in Fig.18.

Fig. 18 shows that the mode shape in the normal condition (Fig.18(a)) has no dominant peak, but has contours which appear to have a similar appearance as those of the damaged membrane (Fig.18(b)). The mode shape in the damaged condition has two dominant peaks, and these two dominant peaks were used to determine the damage positions.

6. Conclusions

In this research, membrane structure damage determination by vibration testing using non-contact laser excitation and a finite element model of the membrane structure were proposed to investigate modelling and damage detection of membrane structures. In addition, a comparison between the simulations and the experimental results confirmed the effectiveness and usefulness of the membrane model and damage detection approach.

The use of the laser excitation vibration measurement arrangement for LIB in this research enabled a high degree of measurement reproducibility, and experiments with very small extents of damage; offering the promise that the quality and reliability of membrane structure damage detection methodology can be improved with the proposed approach. Both the simulations and experimental results for the membrane structure damage detection showed that different types and positions of damage in the membrane can be effectively identified by using the 2-D CWT and the iso-surface concept, which requires only mode shapes of membrane in the application they are used. Vibration testing using acoustic excitation by LIB offers the possibility of detecting the position of damage in membrane structure using both low frequency data (first principal mode shape) and high frequency data (high order mode shape).

Acknowledgements

This study was supported by the Grant-in-Aid for Scientific Research (A) (22246027), Grant-in-Aid for Challenging Exploratory Research (24656158) and Grant-in-Aid for Young Scientists (A) (22686025) from the Japan Society for the Promotion of Science. We hereby express our deep gratitude for this support.

References

- [1] C.H. Jenkins, Membrane vibration experiments: An historical review and recent results, *Journal of Sound and Vibration* 295 (2006) 602 – 613.
- [2] V.A. Chobotov, R.C. Binder, Nonlinear response of a circular membrane to sinusoidal acoustic excitation, *Journal of Acoustical Society of America* 36 (1964) 59–73.
- [3] C.H. Jenkins, Membrane vibrations: a review and new experimental results, in: *ASME Joint Applied Mechanics and Materials Summer Conference*, Blacksburg, VA, 1999.
- [4] C.H. Jenkins, M. Tampi, Local membrane vibrations and inflatable space structures, in: S.W. Johnson, K.M. Chua, R.G. Galloway, P.I. Richler (Eds.), *Space 2000*, Albuquerque, NM, 2000.

- [5] N. Hosoya, M. Nagata, I. Kajiware, Acoustic testing in a very small space based on a point sound source generated by laser-induced breakdown: Stabilization of plasma formation, *Journal of Sound and Vibration* 332 (2013) 4572 – 4583.
- [6] I. Kajiware, K. Obara, Laser excitation vibration test for membrane structures in vacuum environment, *The Sixth Japan-Taiwan Workshop on Mechanical and Aerospace Engineering*, Sapporo, Hokkaido, Japan, 2011.
- [7] M. Oksanen, J. Hietanen, Photo acoustic breakdown sound source in air, *Journal of Ultrasonics* 32 (1994) 327–33.
- [8] Q. Qin, K. Attenborough, Characteristics and application of laser-generated acoustic shock waves in air, *Journal of Applied Acoustics* 65 (2004) 325–340.
- [9] V.B. Georgiev, V.V. Krylov, Q. Qin, K. Attenborough, Generation of flexural waves in plates by laser-initiated air borne shock waves, *Journal of Sound and Vibration* 330 (2011) 217–228.
- [10] J.P. Antoine, R. Murenzi, P. Vandergheynst, *Two-dimensional wavelets and their relatives*, Cambridge University Press, Cambridge, 2004.
- [11] L. Jacques, A. Coron, P. Vandergheynst, A. Rivoldini, The YAWTb Toolbox: Yet Another Wavelet Toolbox, web page: <http://sites.uclouvain.be/ispgroup/yawtb> .
- [12] W. Fan, P. Qiao, A 2-D continuous wavelet transform of mode shape data for damage detection of plate structures, *International Journal of Solids and Structures* 46 (2009) 4379-4395.
- [13] F. Huda, I. Kajiware, N. Hosoya, S. Kawamura, Bolt loosening analysis and diagnosis by non-contact laser excitation vibration tests, *Journal of Mechanical Systems and Signal Processing* 40 (2013) 589-604.
- [14] I. Kajiware, and N. Hosoya, Vibration testing based on impulse response excited by laser ablation, *Journal of Sound and Vibration* 330 (2011) 5045 - 5057.
- [15] N. Hosoya, I. Kajiware, T. Hosokawa, Vibration testing based on impulse response excited by pulsed-laser ablation: measurement of frequency response function with detection-free input, *Journal of Sound and Vibration* 331 (2012) 1355 - 1365.
- [16] I. Kajiware, D. Miyamoto, N. Hosoya, C. Nishidome, Structural health monitoring by high frequency vibration measurement with non-contact laser excitation, *Proceedings of SPIE Smart Structures/NDE 2011* (2011) No. 7984-54.

- Fig. 1 Process to achieve acoustic excitation by LIB
- Fig. 2 Acoustic excitation of a membrane structure by LIB
- Fig. 3 Vibration testing apparatus and arrangement for the membrane structure
- Fig. 4 Finite element model of the membrane structure (with forces and meshing elements)
- Fig. 5 Process of the analysis of the membrane in normal condition by simulation data (a) first principal mode shape (41.8 Hz), (b) interpolated first principal mode shape, (c) wavelet coefficient, (d) wavelet coefficient with boundary treatments
- Fig. 6 Finite element model of membrane with damage scenarios detailed in Table 1
- Fig. 7 Process of the analysis for detecting the L-cut damage (A in Table 1) on the membrane by simulation data (a) first principal mode shape (41.78 Hz), (b) interpolated first principal mode shape, (c) wavelet coefficient, (d) wavelet coefficient with boundary treatment, (e) 3-D view of iso-surface, (f) top view of iso-surface
- Fig. 8 Iso-surface view of the detected L-tear damage (B in Table 1) on the membrane by simulation data (a) 3-D view of iso-surface, (b) top view of iso-surface
- Fig. 9 Analysis of first principal mode shape for detecting the I-cut damage (C in Table 1) on the membrane by simulation data (a) first principal mode shape (41.79 Hz), (b) wavelet coefficient with boundary treatment
- Fig. 10 Analysis of higher order mode shape for detecting the I-cut damage (C in Table 1) on the membrane by simulation data (a) mode shape (851 Hz), (b) wavelet coefficient with boundary treatment, (c) 3-D view of iso-surface, (d) top view of iso-surface
- Fig. 11 Frequency response of the membrane in the normal condition at centre of membrane
- Fig. 12 Process of the analysis for detecting the L-cut damage (A in Table 1) on membrane by experimental data (a) first principal mode shape (40.63 Hz), (b) interpolated first principal mode shape, (c) wavelet coefficient, (d) wavelet coefficient with boundary treatment, (e) 3-D view of iso-surface, (f) top view of iso-surface
- Fig. 13 Iso-surface view of the detected L-tear damage (B in Table 1) on the membrane by experimental data (a) 3-D view of iso-surface, (b) top view of iso-surface
- Fig. 14 Analysis of higher order mode shape for detecting the I-cut damage (C in Table 1) on the membrane by experimental data (a) mode shape (843.8 Hz), (b) wavelet coefficient with boundary treatment, (c) 3-D view of iso-surface, (d) top view of iso-surface
- Fig. 15 Membrane with I-cut and square-hole damage
- Fig. 16 Process of the analysis for detecting I-cut and square-hole damage on the membrane by experimental data (a) mode shape (799.1 Hz), (b) wavelet coefficient with boundary treatment, (c) 3-D view of iso-surface, (d) top view of iso-surface
- Fig. 17 Frequency response of membrane without induced damage and condition with damage in two places
- Fig. 18 Plots of the two mode shapes (a) mode shape w/o induced damage (801.6 Hz), (b) mode shape with damage in two places (799.1 Hz)

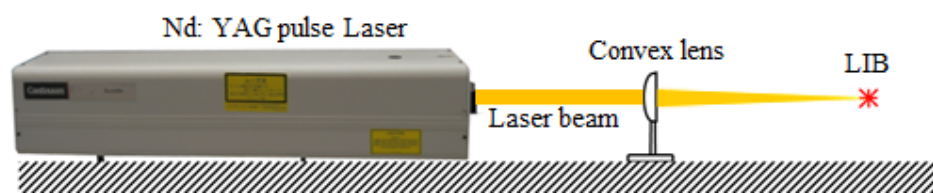


Fig. 1 Process to achieve acoustic excitation by LIB

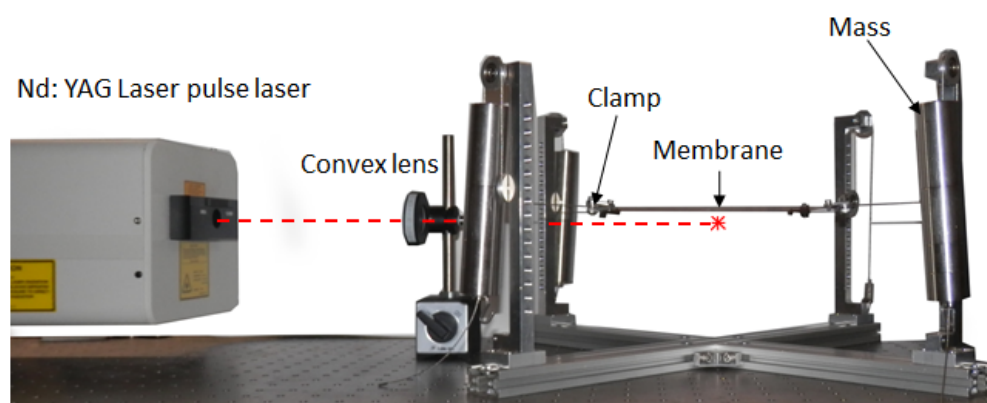


Fig. 2 Acoustic excitation of a membrane structure by LIB

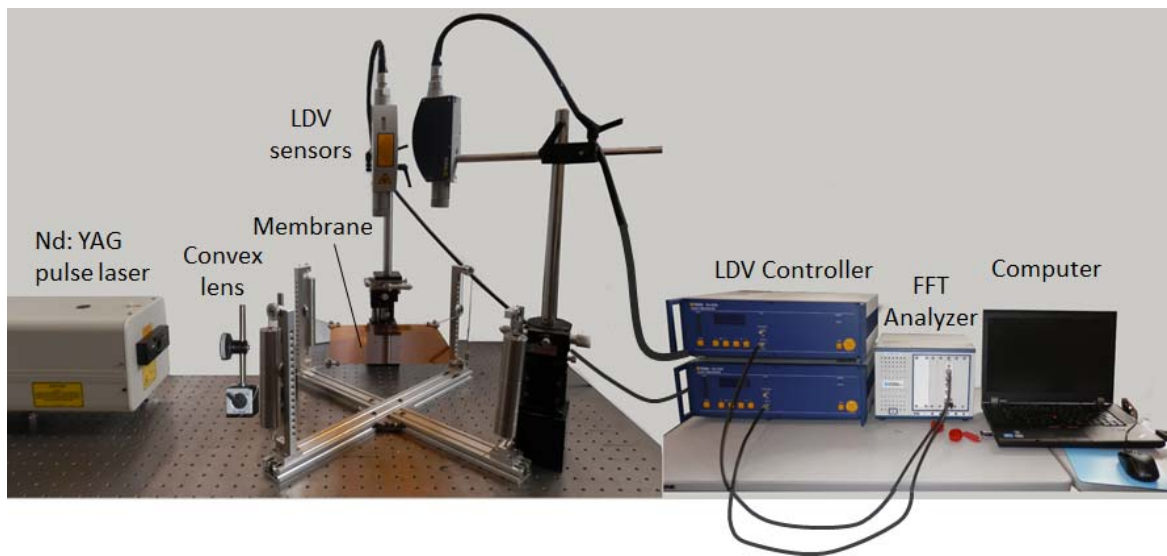


Fig. 3 Vibration testing apparatus and arrangement for the membrane structure

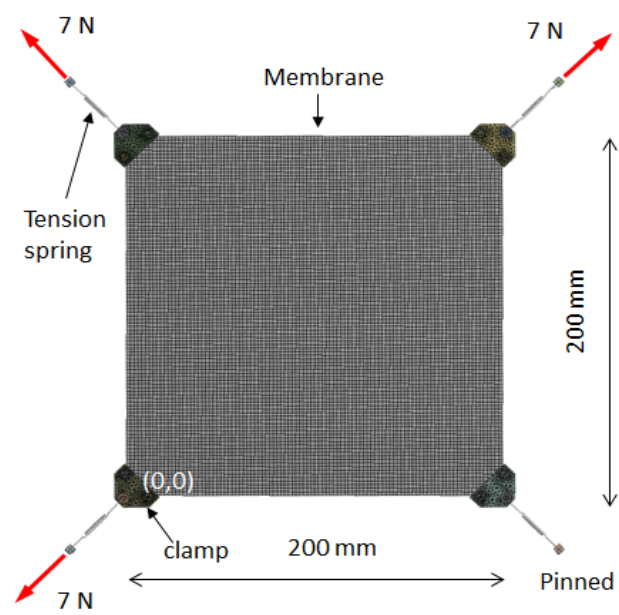
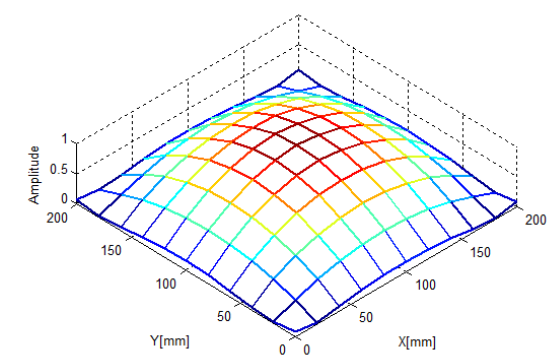
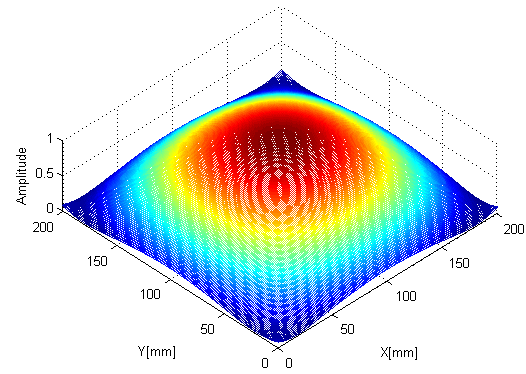


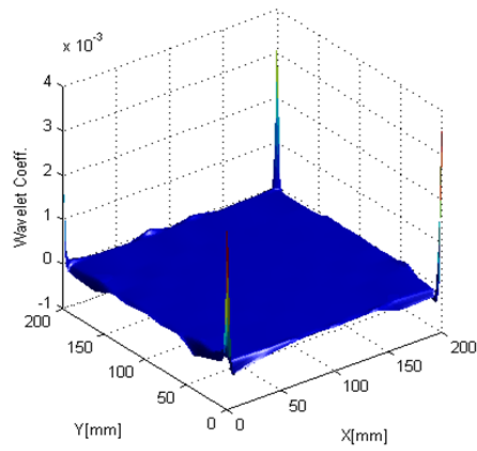
Fig. 4 Finite element model of the membrane structure (with forces and meshing elements)



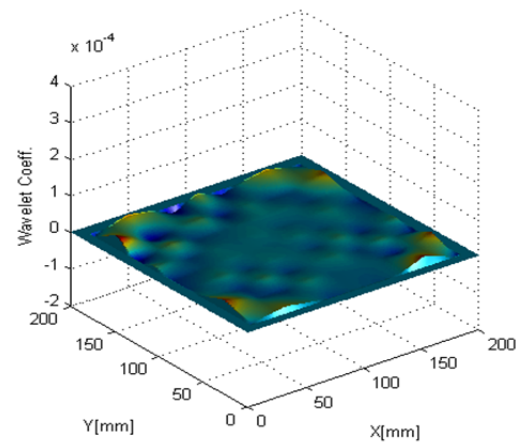
(a)



(b)



(c)



(d)

Fig. 5 Process of the analysis of the membrane in normal condition by simulation data (a) first principal mode shape (41.8 Hz), (b) interpolated first principal mode shape, (c) wavelet coefficient, (d) wavelet coefficient with boundary treatments

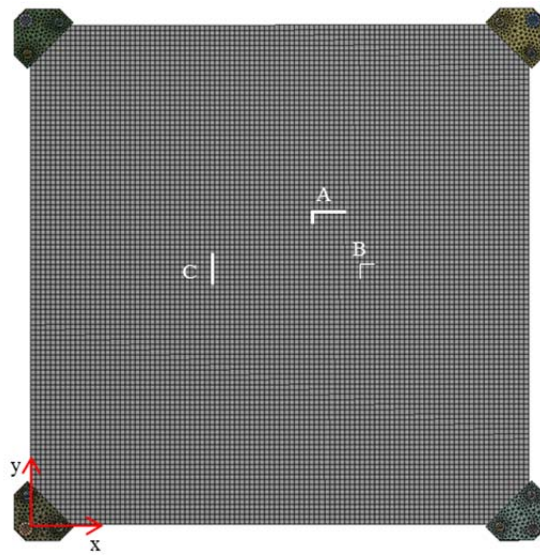


Fig. 6 Finite element model of membrane with damage scenarios detailed in Table 1

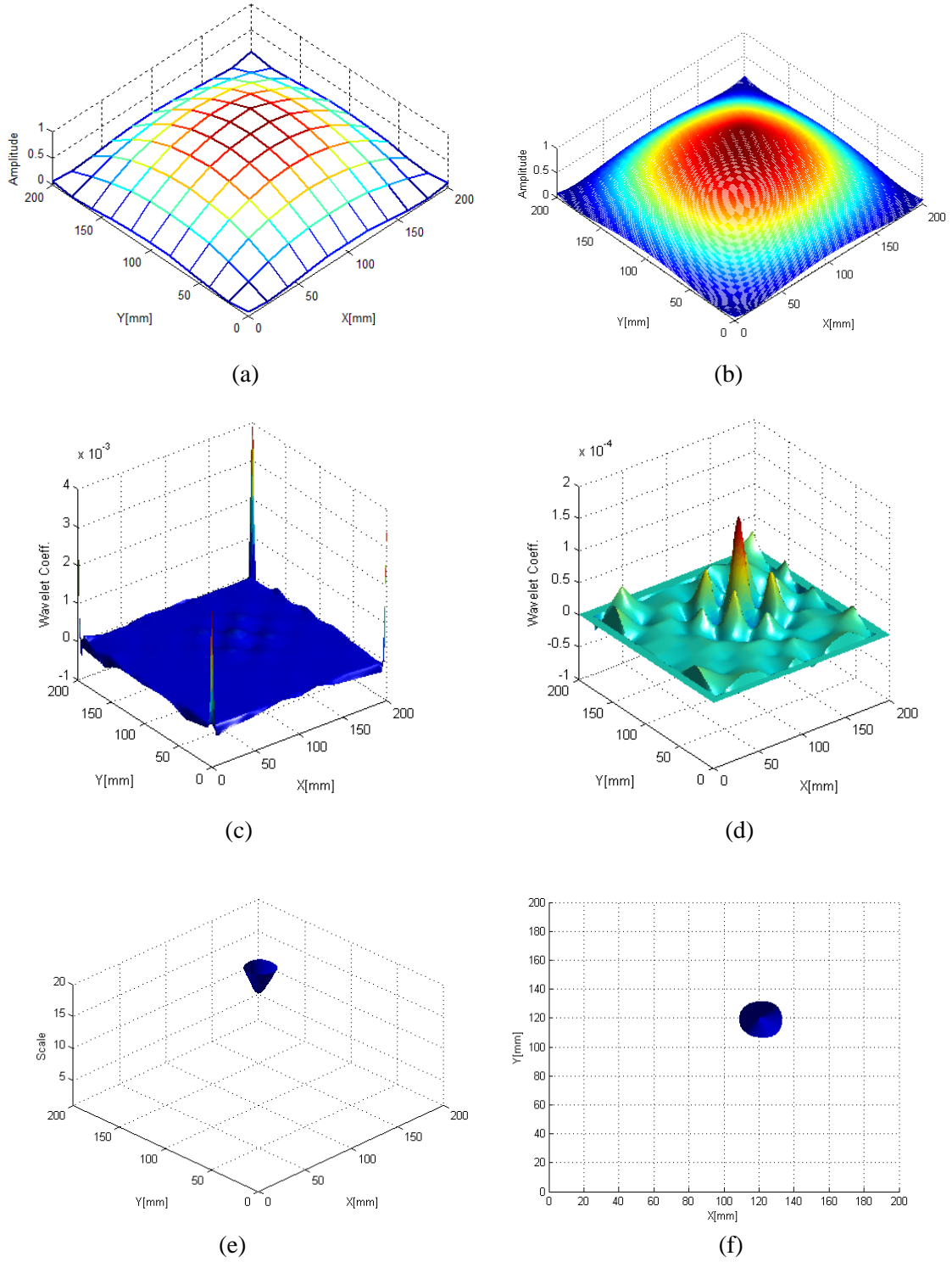
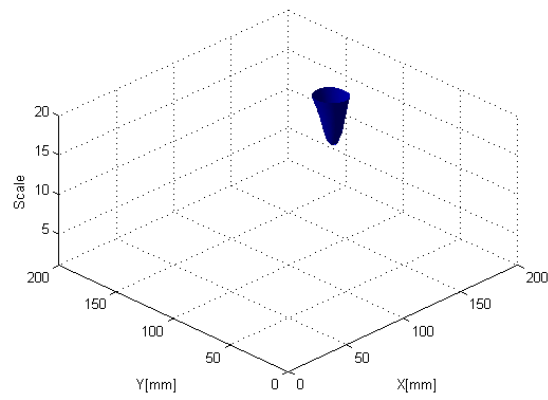
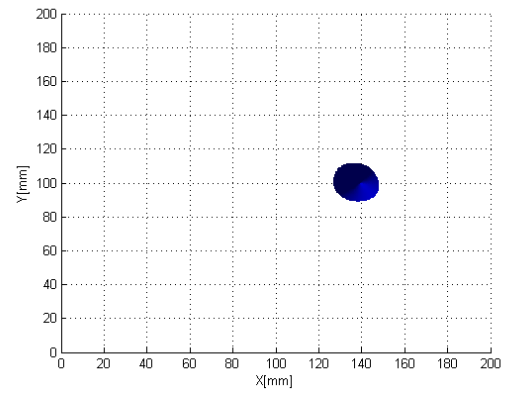


Fig. 7 Process of the analysis for detecting the L-cut damage (A in Table 1) on the membrane by simulation data (a) first principal mode shape (41.78 Hz), (b) interpolated first principal mode shape, (c) wavelet coefficient, (d) wavelet coefficient with boundary treatment, (e) 3-D view of iso-surface, (f) top view of iso-surface

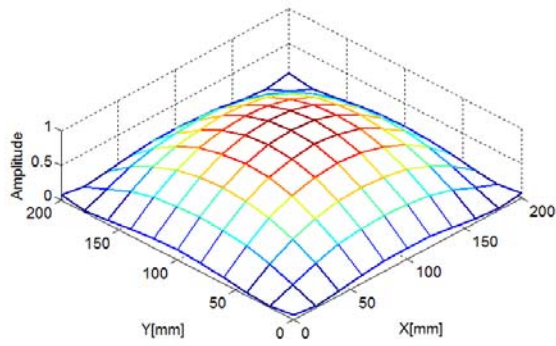


(a)

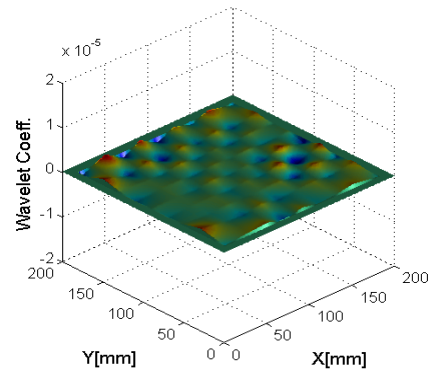


(b)

Fig. 8 Iso-surface view of the detected L-tear damage (B in Table 1) on the membrane by simulation data (a) 3-D view of iso-surface, (b) top view of iso-surface



(a)



(b)

Fig. 9 Analysis of first principal mode shape for detecting the I-cut damage (C in Table 1) on the membrane by simulation data (a) first principal mode shape (41.79 Hz), (b) wavelet coefficient with boundary treatment

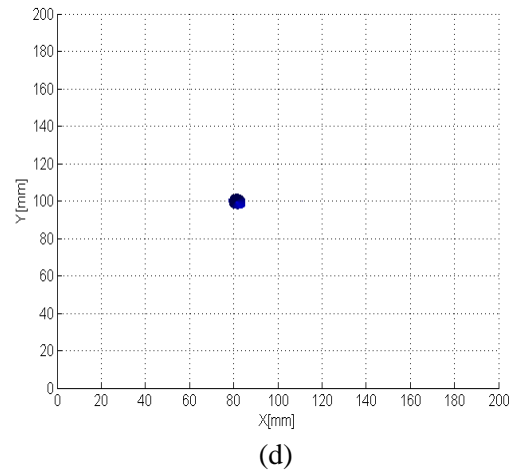
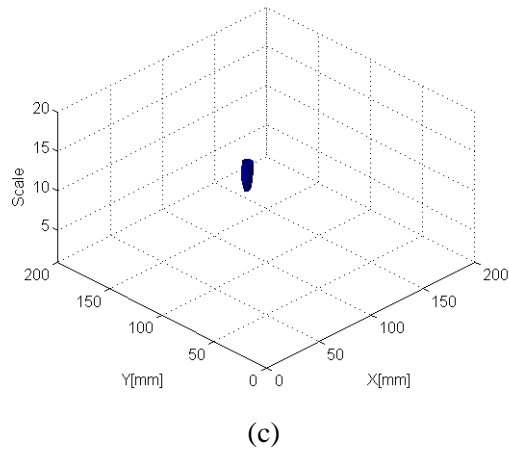
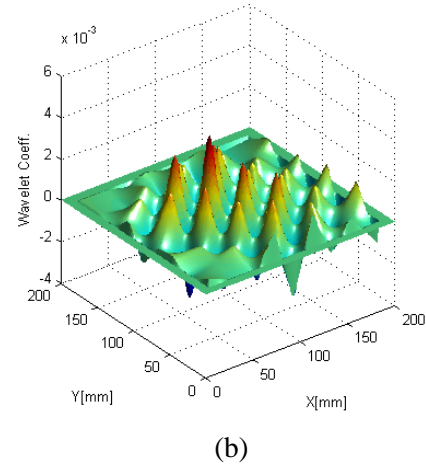
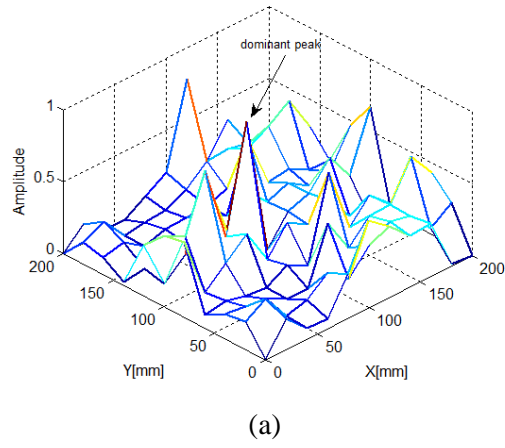


Fig. 10 Analysis of higher order mode shape for detecting the I-cut damage (C in Table 1) on the membrane by simulation data (a) mode shape (851 Hz), (b) wavelet coefficient with boundary treatment, (c) 3-D view of iso-surface, (d) top view of iso-surface

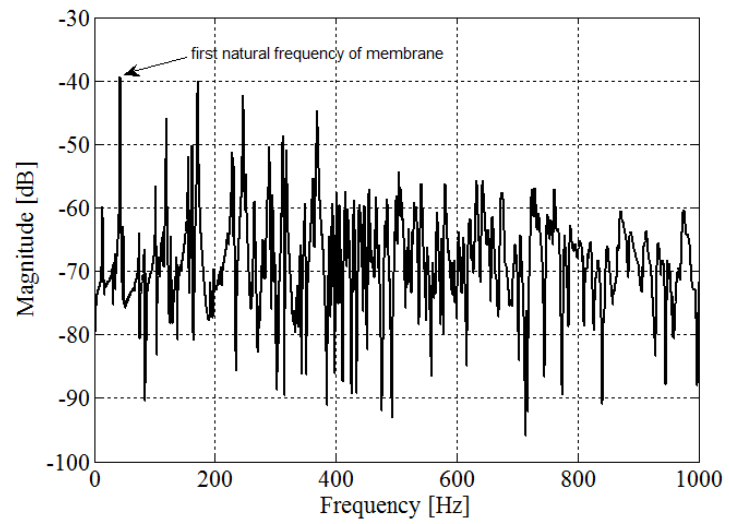
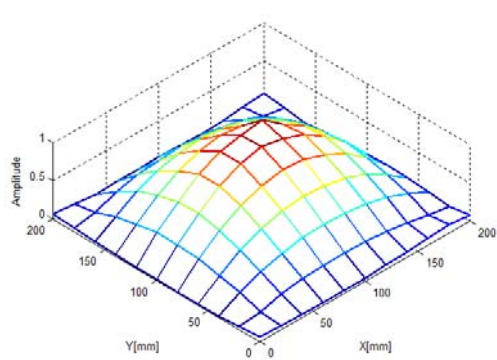
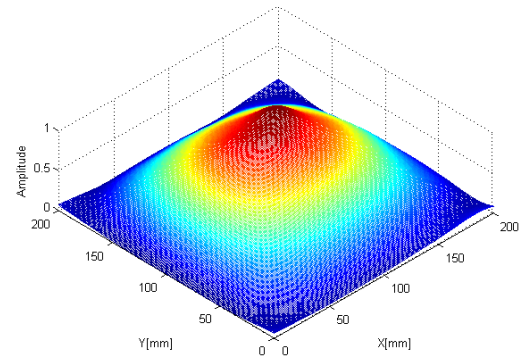


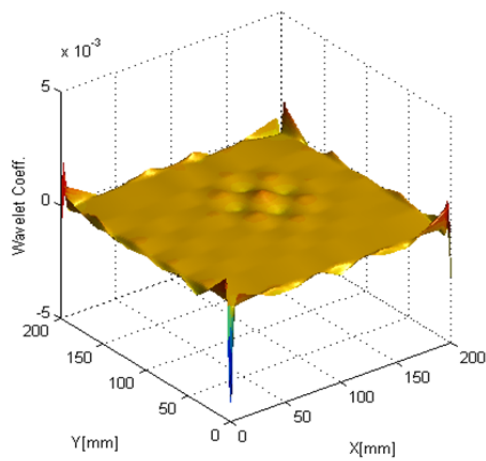
Fig. 11 Frequency response of the membrane in the normal condition at centre of membrane



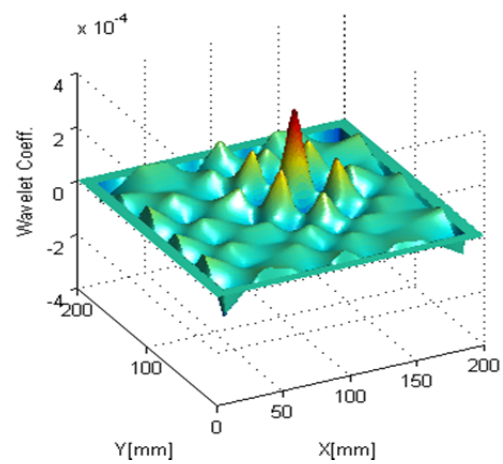
(a)



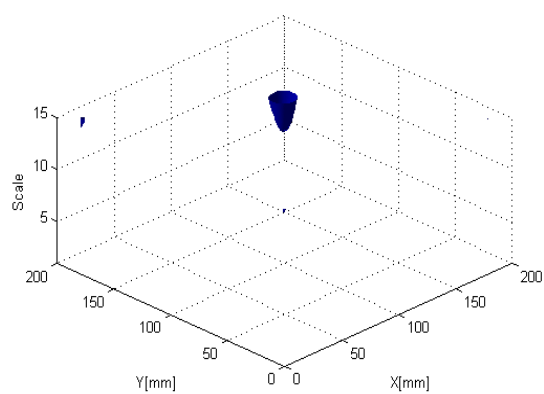
(b)



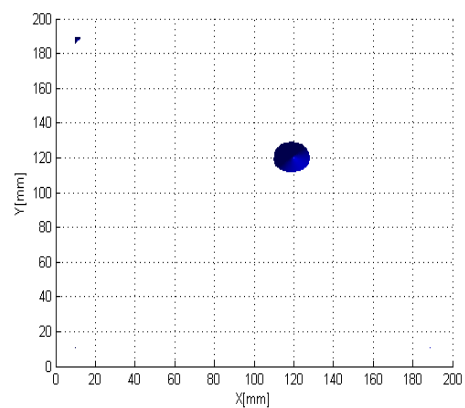
(c)



(d)



(e)



(f)

Fig. 12 Process of the analysis for detecting the L-cut damage (A in Table 1) on membrane by experimental data (a) first principal mode shape (40.63 Hz), (b) interpolated first principal mode shape, (c) wavelet coefficient, (d) wavelet coefficient with boundary treatment, (e) 3-D view of iso-surface, (f) top view of iso-surface

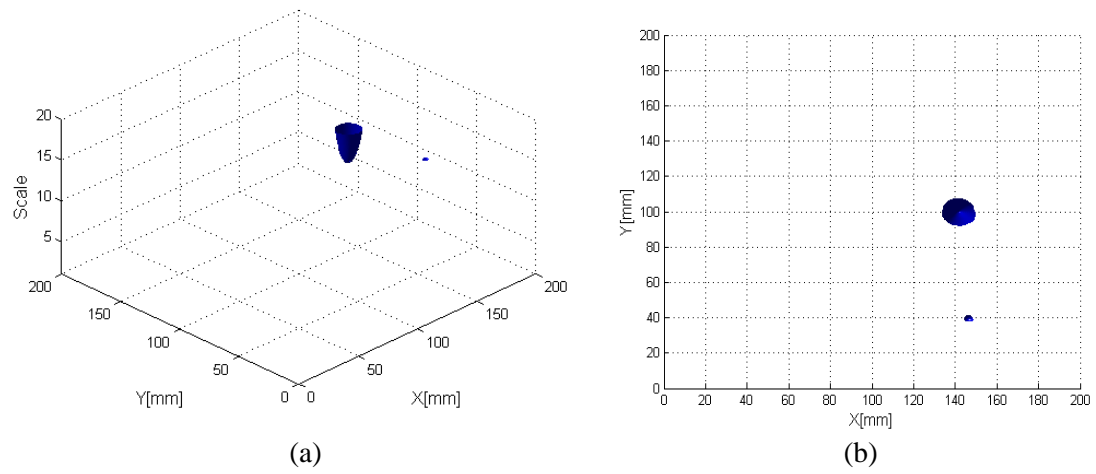


Fig. 13 Iso-surface view of the detected L-tear damage (B in Table 1) on the membrane by experimental data (a) 3-D view of iso-surface, (b) top view of iso-surface

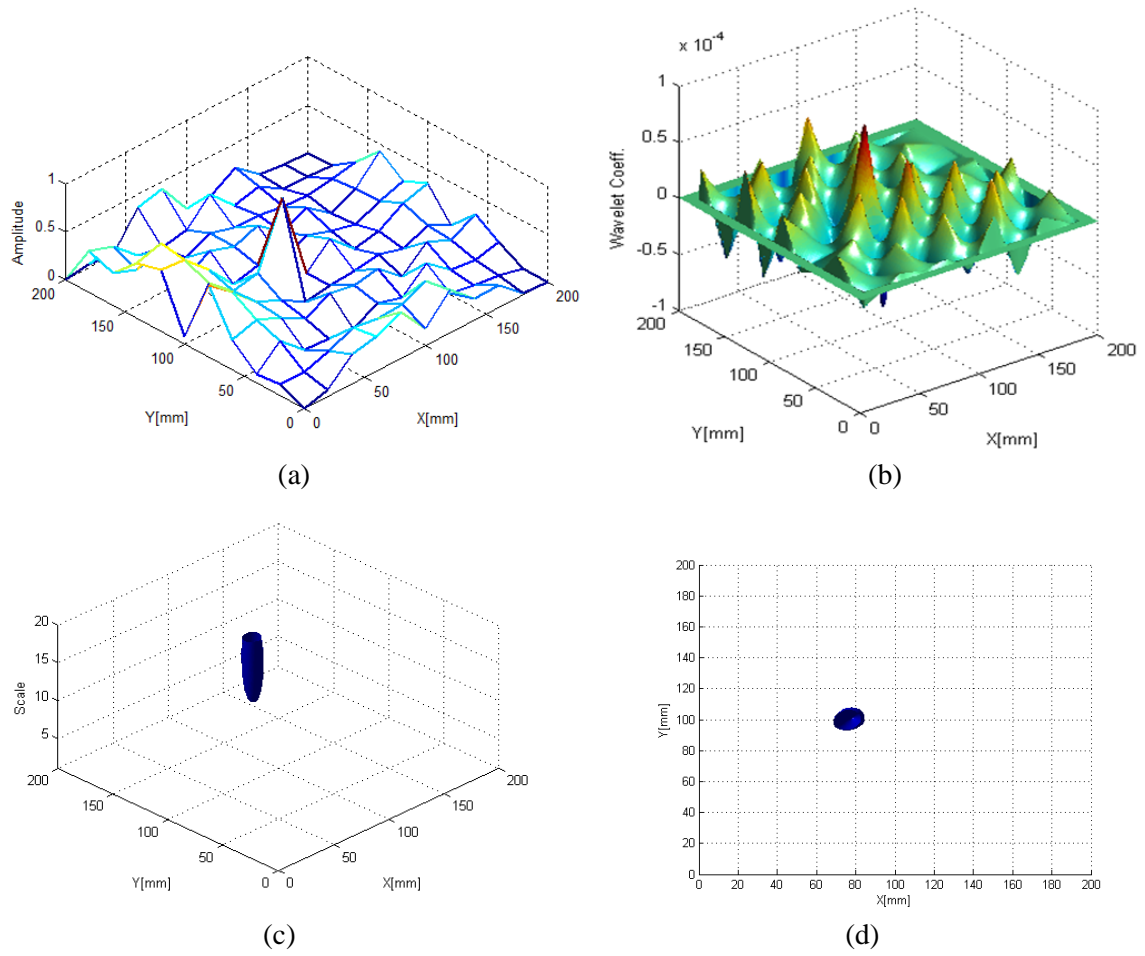


Fig. 14 Analysis of higher order mode shape for detecting the I-cut damage (C in Table 1) on the membrane by experimental data (a) mode shape (843.8 Hz), (b) wavelet coefficient with boundary treatment, (c) 3-D view of iso-surface, (d) top view of iso-surface

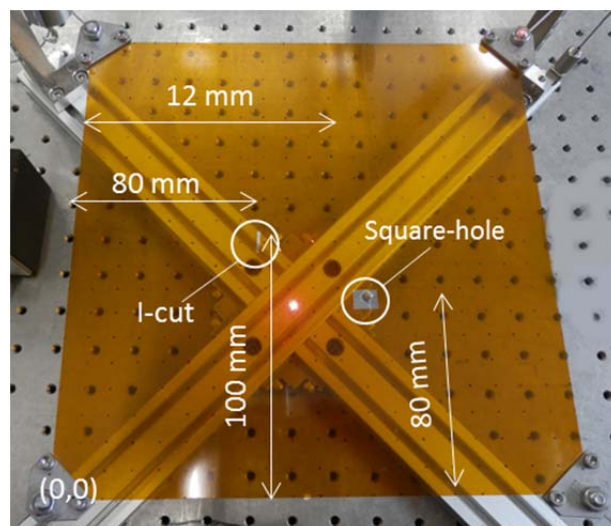
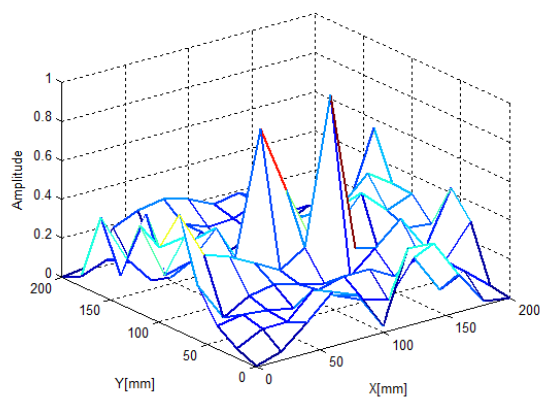
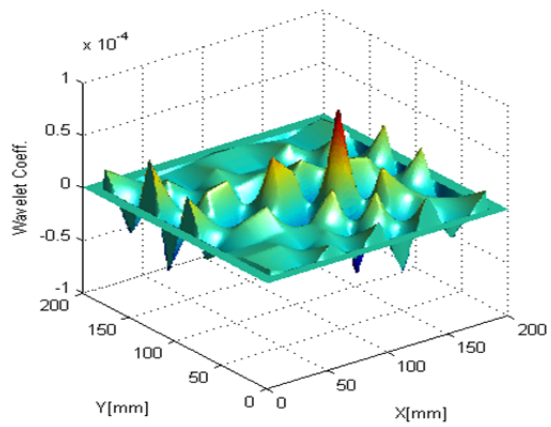


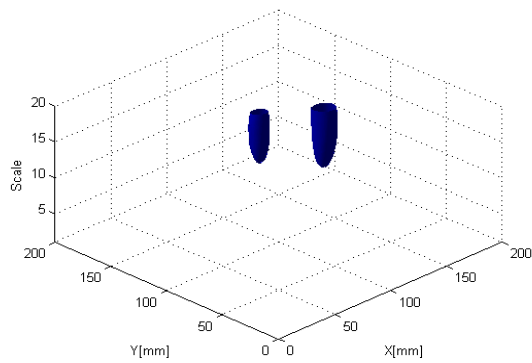
Fig. 15 Membrane with I-cut and square-hole damage



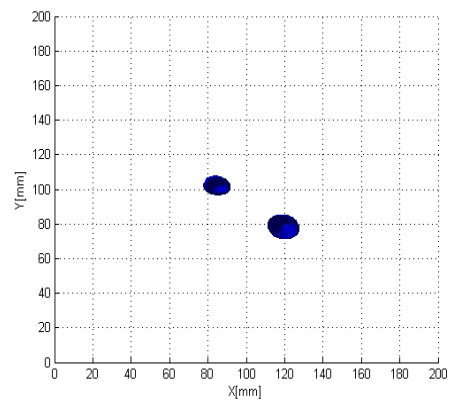
(a)



(b)



(c)



(d)

Fig. 16 Process of the analysis for detecting I-cut and square-hole damage on the membrane by experimental data (a) mode shape (799.1 Hz), (b) wavelet coefficient with boundary treatment, (c) 3-D view of iso-surface, (d) top view of iso-surface

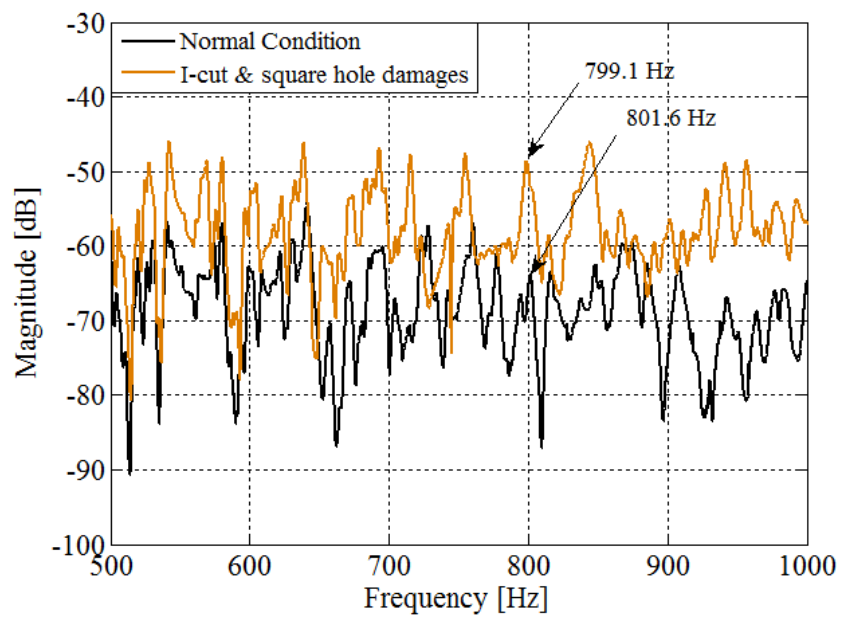


Fig.17 Frequency response of membrane without induced damage and condition with damage in two places

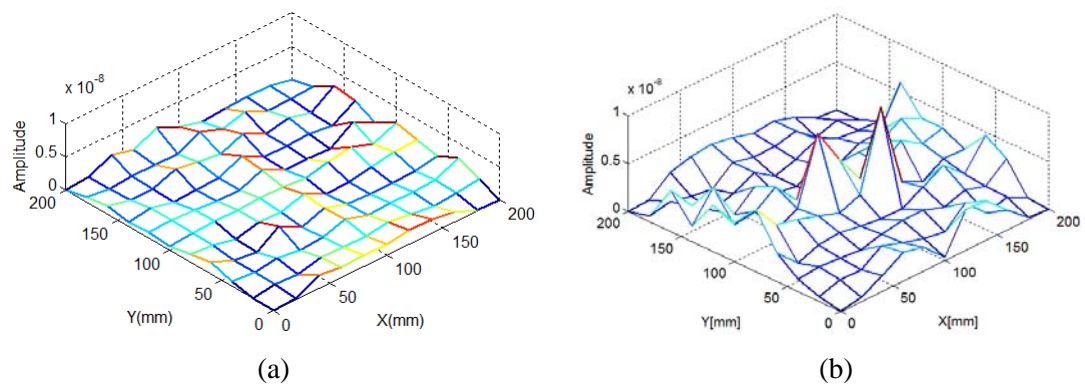


Fig. 18 Plots of the two mode shapes (a) mode shape w/o induced damage (801.6 Hz), (b) mode shape with damage in two places (799.1 Hz)